Journal of Thermal Analysis and Calorimetry, Vol. 83 (2006) 1, 233–240

SYNTHESIS, CHARACTERIZATION AND THERMAL STUDIES ON SOLID COMPOUNDS OF 2-CHLOROBENZYLIDENEPYRUVATE OF HEAVIER TRIVALENT LANTHANIDES AND YTTRIUM(III)

G. Bannach[1], *E. Schnitzler*[2], *O. Treu Filho*[1], *V. H. S. Utuni*[1] *and M. Ionashiro*[1*]

[1]Instituto de Química UNESP, Araraquara SP, CP 355, CEP 14801-970, Brazil
[2]Departamento de Química, UEPG, 84030-000 Ponta Grossa, PR, Brasil

Solid-state compounds of general formula $LnL_3{\cdot}nH_2O$, where *Ln* represents heavier lanthanides and yttrium and *L* is 2-chlorobenzylidenepyruvate, have been synthesized. Chemical analysis, simultaneous thermogravimetry-differential analysis (TG-DTA), differential scanning calorimetry (DSC), X-ray powder diffractometry, elemental analysis and infrared spectroscopy have been employed to characterize and to study the thermal behaviour of these compounds in dynamic air atmosphere.

On heating these compounds decompose in four (Gd, Tb, Ho to Lu, Y) or five (Eu, Dy) steps. They lose the hydration water in the first step and the thermal decomposition of the anhydrous compounds up to 1200°C occurs with the formation of the respective oxide, Tb_4O_7 and Ln_2O_3 (*Ln*=Eu, Gd, Dy to Lu and Y) as final residue. The dehydration enthalpies found for these compounds (Eu, to Lu and Y) were: 65.77, 55.63, 86.89, 121.65, 99.80, 109.59, 131.02, 119.78, 205.46 and 83.11 kJ mol^{-1}, respectively.

Keywords: *benzylidenepyruvate, rare earth, thermal behaviour*

Introduction

Synthesis of benzylidenepyruvic acid (HBP), as well as of phenyl-substituted derivatives of HBP, has been reported [1, 2]. These acids are of continuing interest as intermediates in pharmacological, industrial and chemical syntheses, in the development of enzyme inhibitors and drugs, as model substrates of enzymes, and in other ways [3–7].

Preparation and investigation of several metal-ion complexes of phenyl-substituted derivatives of BP, have been carried out in aqueous solutions [8–10], and in solid-state [11–19]. In aqueous solutions these works reported mainly the thermodynamic stability (β_1) and spectroscopic parameters (ε_{1max}, λ_{max}), associated with 1:1 complex species, analytical applications of the ligands, e.g., in gravimetric analysis and as metallochromic indicators, while in the solid-state, the establishment of the stoichiometry and detailed knowledge of the thermal behaviour of the ligands and their metal ion compounds have been the main purposes of these studies.

In the present paper, ligand and solid-state compounds of heavier trivalent lanthanides and yttrium(III) with 2-chlorobenzylidenepyruvate, $2\text{-Cl–}C_6H_4\text{–CH=CH–CO–COO}^-$, were synthesized. The compounds were investigated by means of chemical analysis, X-ray powder diffractometry, elemental analysis (E. A.), infrared spectroscopy, differential scanning calorimetry (DSC) and simultaneous thermogravimetry and differential thermal analysis (TG-DTA). The data obtained allowed us to acquire information concerning these compounds in the solid-state, including their thermal behaviour and thermal decomposition.

Experimental

Sodium 2-chlorobenzylidenepyruvate and its corresponding acid were synthesized following the same procedure described in the literature [17], with some modification as follows: an aqueous solution of sodium pyruvate (22 g per 50 mL) was added with continuous stirring, to 24 mL of 2-chlorobenzaldehyde (29 g). Sixty milliliters of an aqueous sodium hydroxide solution (18 *m*/*v*%) was slowly added while the reacting system was stirred and cooled in an ice-bath. The rate of addition of alkali was regulated so that the temperature remained between 5 and 9°C. The formation of a pale yellow precipitate was observed during the addition of the sodium hydroxide solution.

The system is left to stand for about 3 h at room temperature (23–28°C). The pale yellow precipitate (impure sodium 2-chlorobenzylidenepyruvate) is filtered, washed with five 100 mL portions of methanol, to remove most of the unreacted aldehyde and secondary products. The crude product was dissolved in water (500 mL) and aldehyde yet present as contaminating was removed through a separator funnel.

* Author for correspondence: massaoi@iq.unesp.br

1388–6150/$20.00

Akadémiai Kiadó, Budapest, Hungary
Springer, Dordrecht, The Netherlands

In the sodium 2-chlorobenzylidenepyruvate solution was added under continuous stirring, concentrated (12 mol L^{-1}) hydrochloric acid until total precipitation of the 2-chlorobenzylidenepyruvic acid (12.3 g).

Aqueous solution of Na2-Cl-BP, 0.1 mol L^{-1} was prepared by direct weighing of the salt. Lanthanide chlorides were prepared from the corresponding metal oxides (except for yttrium) by treatment with concentrated hydrochloric acid. The residues were dissolved in distilled water, transferred to a volumetric flask and diluted in order to obtain ca. 0.1 mol L^{-1} solutions, whose pH were adjusted to 5.0 by adding diluted sodium hydroxide or hydrochloric acid solutions. Yttrium(III) was used as its chloride and 0.1 mol L^{-1} aqueous solutions of this ion were prepared by direct weighing of the salt.

The solid-state compounds Ln(2-Cl-BP)$_3$ (*Ln*= lanthanides or yttrium) were prepared by adding slowly, with continuous stirring, the solutions of the ligand to the respective metal chloride solutions, until total precipitation of the metal ions. The precipitates were washed with distilled water until elimination of the chloride ions, filtered through and dried on Whatman n° 42 filter paper, and kept in a desiccator over anhydrous calcium chloride.

In solid-state compounds, hydration water, ligand and metal contents were determined from the TG curves. The metal ions were also determined by complexometric titrations with standard EDTA solutions, using xylenol orange as indicator [20].

X-ray powder patterns were obtained by using a Siemens D-5000 X-ray diffractometer, employing CuK_α radiations (λ=1.541 Å) and setting of 40 kV and 20 mA.

Infrared spectra for 2-Cl-BP (sodium salt) as well as for its trivalent lanthanide compounds were run on a Nicolet mod. Impact 400 FTIR instruments, within 4000–400 cm^{-1} range. The solid samples were pressed into KBr pellets.

Carbon and hydrogen contents were determined by microanalytical procedures, with an EA 1110 CHNS-O Elemental Analyzer from CE Instruments.

Simultaneous TG-DTA curves were obtained with thermal analysis system, model SDT 2960, from TA Instruments. The purge gas was an air flow of 100 mL min^{-1}. A heating rate of 20°C min^{-1} was adopted, with samples weighing about 9 mg. Alumina crucible, was used for TG-DTA curves.

The DSC curves were obtained using a Mettler TA-4000 thermal analysis system with an air flux of 100 mL min^{-1}, a heating rate of 20°C min^{-1} and with samples weighing about 5 mg. Aluminium crucible with perforated cover was used for DSC curves.

The final thermal decomposition residues up to 580°C (Eu, Yb); 550°C (Gd, Tb, Dy, Tm); 530°C (Ho, Lu, Y) and 520°C (Er) were characterized by X-ray powder diffractometry.

Computational strategy

For calculation of theoretical infrared spectrum of yttrium 2-chlorobenzylidenepyruvate it is necessary to evaluate the structure and wave function computed by the ab initio SCF Hartree–Fock–Roothan method [21] using a split valence (3–21 g*) basis set [22]. The performed molecular calculations in this work were done by using the Gaussian 98 routine [23] and the hardware used is the IBM power 3. The crystal geometry of yttrium 2-chlorobenzylidenepyruvate is unknown. The geometry optimization was carried out without any constraints. The molecule of 2-chlorobenzylidenepyruvate contain rings with conformational flexibility, all variables were optimized. The optimization proceeded more uniformly when all variables were optimized.

Results and discussion

The analytical results of the synthesized compounds are shown in Table 1. These data permitted to establish the stoichiometry of the compounds, which is in agreement with general formula Ln(2-Cl-BP)$_3$·*n*H_2O, where

Table 1 Analytical data for Ln(L)$_3$·*n*H_2O

Compound	Water/%		*L*. lost/%		Metal/%			Δ*m* total/%		Carbon/%		Hydrogen/%	
	theor.	TG	theor.	TG	theor.	TG	EDTA	theor.	TG	theor.	E.A.	theor.	E.A.
Eu(L)$_3$·2H_2O	4.41	4.32	74.05	74.04	18.60	18.69	19.03	78.46	78.36	44.11	44.93	2.72	3.03
Gd(L)$_3$·2H_2O	4.38	4.35	73.57	73.46	19.13	19.25	19.06	77.95	77.81	43.83	44.65	2.70	2.83
Tb(L)$_3$·2H_2O	4.37	4.26	72.94	73.25	19.29	19.12	19.19	77.31	77.51	43.74	43.51	2.70	2.61
Dy(L)$_3$·H_2O	2.23	2.41	74.73	74.45	20.08	20.16	20.37	76.96	76.86	44.52	44.71	2.50	2.87
Ho(L)$_3$·3H_2O	6.36	6.25	71.36	71.70	19.45	19.25	19.33	77.72	77.95	42.50	42.25	2.86	2.70
Er(L)$_3$·3H_2O	6.36	6.22	71.14	71.31	19.67	19.65	19.38	77.50	77.53	42.38	42.60	2.85	2.55
Tm(L)$_3$·3H_2O	6.35	6.59	71.00	70.82	19.83	19.78	19.84	77.35	77.41	42.30	41.64	2.85	2.78
Yb(L)$_3$·3H_2O	6.32	6.25	70.66	71.02	20.22	19.96	20.22	76.98	77.27	42.09	41.90	2.83	2.69
Lu(L)$_3$·3H_2O	6.30	6.20	70.51	70.63	20.40	20.38	20.37	76.81	76.83	42.00	41.75	2.83	2.74
Y(L)$_3$·2H_2O	4.78	4.56	80.24	79.97	11.79	12.18	11.66	85.02	84.53	47.80	48.64	2.95	2.66

Ln=lanthanides, *L*=2-chlorobenzylidenepyruvate

Table 2 IR spectroscopic data for sodium 2-chlorobenzylidenepyruvate and for its compounds with heavier trivalent lanthanides

Compound	$\nu_{O-H}H_2O$	$\nu_{s(COO^-)}$	$\nu_{as(COO^-)}$	$\nu_{C=O}$
$NaL\cdot 1.5H_2O$	3443 m	1402 m	1615 s	1682 s
$Eu(L)_3\cdot 2H_2O$	3448 m	1433 m	1589 s	1634 s
$Gd(L)_3\cdot 2H_2O$	3369 m	1427 m	1589 s	1645 s
$Tb(L)_3\cdot 2H_2O$	3385 m	1431 m	1589 s	1651 s
$Dy(L)_3\cdot H_2O$	3443 m	1431 m	1589 s	1645 s
$Ho(L)_3\cdot 3H_2O$	3391 m	1441 m	1585 s	1650 s
$Er(L)_3\cdot 3H_2O$	3369 m	1441 m	1585 s	1651 s
$Tm(L)_3\cdot 3H_2O$	3387 m	1431 m	1587 s	1651 s
$Yb(L)_3\cdot 3H_2O$	3377 m	1431 m	1587 s	1653 s
$Lu(L)_3\cdot 3H_2O$	3394 m	1441 m	1585 s	1651 s
$Y(L)_3\cdot 2H_2O$	3477 m	1429 m	1589 s	1647 s

L=2-chlorobenzylidenepyruvate; s – strong, m – medium, $\nu_{as(O-H)}$ – hydroxyl group stretching frequency; $\nu_{s(COO^-)}$ and $\nu_{as(COO^-)}$ – symmetrical and anti-symmetrical vibrations of the COO^- structure; $\nu_{s(C=O)}$ – ketonic carbonyl stretching frequency

Table 3 Theoretical geometries parameters of yttrium(III) with 2-chlorobenzylidenepyruvate

d O–Y	2.17 Å
d =O–Y	2.36 Å
d C–O	1.29 Å
d YOC=O	1.21 Å
d C=O	1.24 Å
d C–Cl	1.75 Å
< O–Y–O	67.71°
< Y–O–C	128.43°
< Y–O=C	120.18°
< O–C–C	109.25°
< O=C–C	114.42°

d – distance, < – means angle

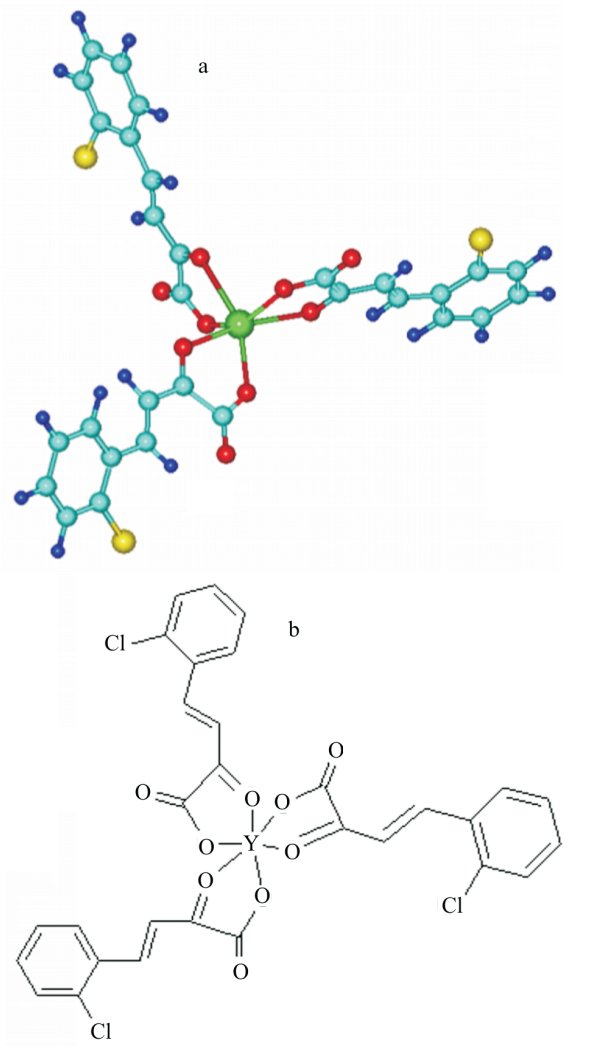

Fig. 1 Proposed structure a – 3D and b – 2D of solid-state compound yttrium(III) with 2-chlorobenzylidenepyruvate was 3D optimized using Hartree–Fock–Roothan method, split-valence (3–21 g*) basis set of Gaussian 98

Ln represents heavier lanthanides (Eu to Lu and Y), 2-Cl-BP is 2-chlorobenzylidenepyruvate and *n*=1 (Dy), 2 (Eu, Gd, Tb, Y), 3 (Ho, Er, Tm, Yb, Lu).

X-ray powder patterns showed that all the compounds were obtained in amorphous state. The amorphous state is undoubtedly related to the low solubility of these compounds, as already observed for lanthanides and yttrium compounds with DMBP [12] and heavier lanthanides and yttrium compounds with 4-MeO-BP and 4-Cl-BP [11, 14].

Infrared spectroscopic data on 2-chlorobenzylidenepyruvate (sodium salt) and its compounds with heavier trivalent lanthanides are shown in Table 2. The bands found for 2-Cl-BP (sodium salt) centered at 1682 cm^{-1} (ketonic carbonyl stretching) and 1615 cm^{-1} (anti-symmetrical carboxylate vibration) are both shifted to lower frequencies in the compounds, namely, 1634–1651 and 1585–1589 cm^{-1}, respectively, suggesting lanthanides coordination by the α-ketonic carbonyl and carboxylate groups of the ligand [24, 25]. This behaviour is in agreement with 4-Me-BP compounds with the same metal ions [15].

The theoretical infrared spectrum of the $Y(L)_3\cdot 3H_2O$ was calculated by using a harmonic field [26] and the obtained frequencies were not scaled. The geometry optimization was computed by the optimized algorithm of Berny [27]. The obtained geometry from calculations is presented in Fig. 1 and Table 3.

The theoretical infrared spectrum (electronic state ^1A) was obtained with frequency values (cm^{-1}), relative intensities, assignments and description of vibrational modes.

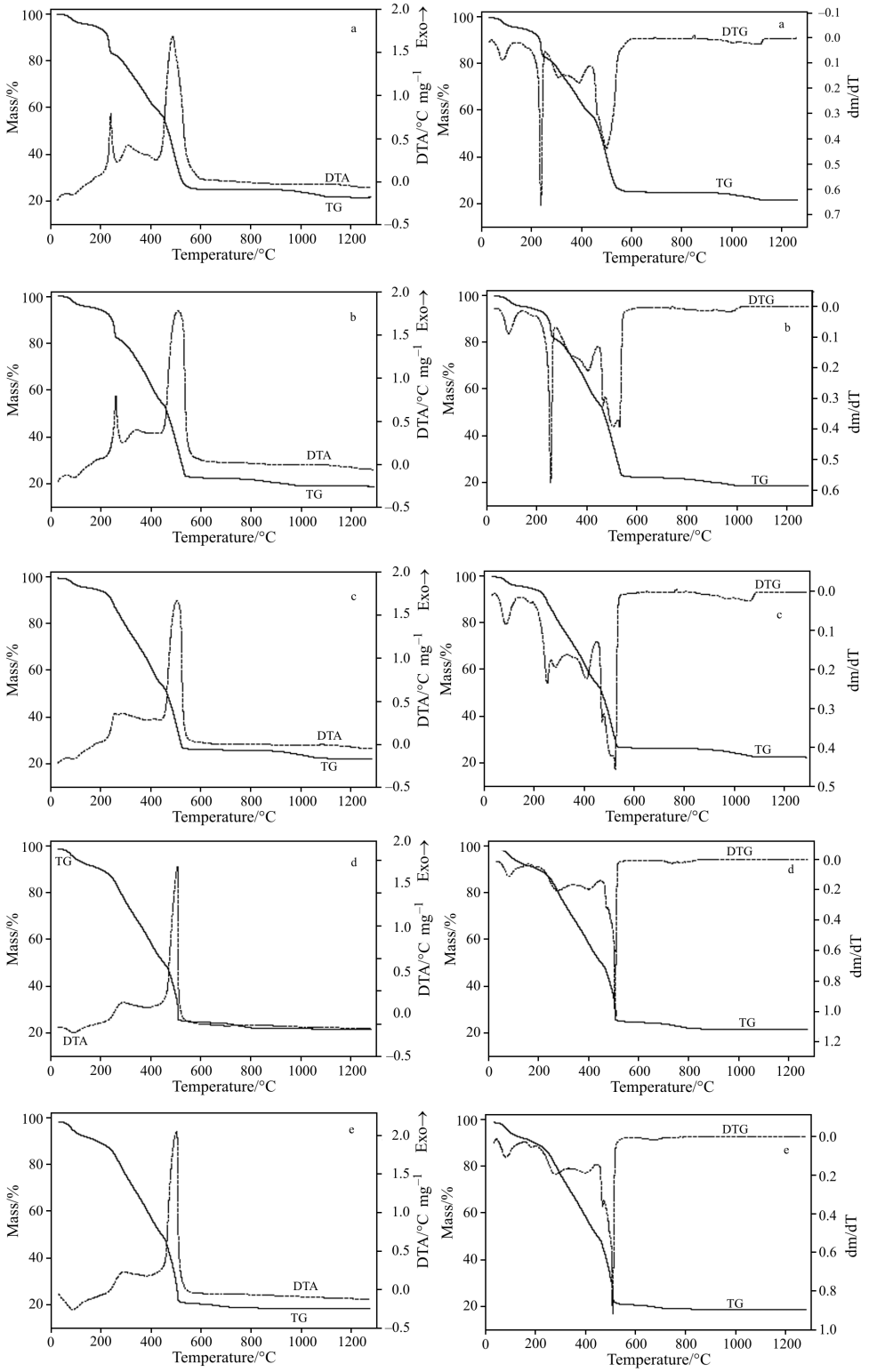

Fig. 2 Simultaneous TG-DTA and TG-DTG curves of the compounds: a – $Eu(2\text{-Cl-BP})_3 \cdot 2H_2O$ (m_i=8.871 mg), b – $Dy(2\text{-Cl-BP})_3 \cdot H_2O$ (10.397 mg), c – $Gd(2\text{-Cl-BP})_3 \cdot 2H_2O$ (8.821 mg), d – $Ho(2\text{-Cl-BP})_3 \cdot 3H_2O$ (9.159 mg) and e – $Lu(2\text{-Cl-BP})_3 \cdot 3H_2O$ (9.714 mg)

A comparative analysis between the experimental and theoretical spectrum shows the following conclusions: (a) the first assignment shows a strong contribution at 1647 cm^{-1} suggesting an ν(C=O) of carbonyl, while the theoretical results show the corresponding peak at 1737 cm^{-1} with discrepancies +5.46%. (b) The second assignment shows a strong contribution at

Table 4 Temperature ranges θ, mass losses and peak temperatures observed for each step of the TG-DTA curves of the compounds

Compound		Steps				
		first	second	third	fourth	fifth
$Eu(L)_3 \cdot 2H_2O$	θ°C	30–140	140–245	245–450	450–600	700–1130
	loss/%	4.32	12.43	27.29	31.07	3.25
	peak/°C	88 (endo)	241 (exo)	311 (exo)	488 (exo)	
$Gd(L)_3 \cdot 2H_2O$	θ°C	30–140	140–455	455–600	800–1070	
	loss/%	4.35	43.53	26.12	3.81	
	peak/°C	90 (endo)	260 (exo)	503 (exo)		
$Tb(L)_3 \cdot 2H_2O$	θ°C	30–140	140–460	460–540	750–980	
	loss/%	4.26	42.90	27.13	3.22	
	peak/°C	90 (endo)	260 (exo)	505 (exo)		
$Dy(L)_3 \cdot H_2O$	θ°C	30–140	140–255	255–455	455–550	700–1000
	loss/%	2.41	12.91	29.67	28.30	3.57
	peak/°C	90 (endo)	255 (exo)	340 (exo)	500 (exo)	
$Ho(L)_3 \cdot 3H_2O$	θ°C	30–140	140–470	470–530	650–830	
	loss/%	6.25	45.63	23.90	2.17	
	peak/°C	95 (endo)	290 (exo)	505 (exo)		
$Er(L)_3 \cdot 3H_2O$	θ°C	30–140	140–455	455–520	600–780	
	loss/%	6.22	44.77	24.13	2.41	
	peak/°C	90 (endo)	280 (exo)	495 (exo)		
$Tm(L)_3 \cdot 3H_2O$	θ°C	30–140	140–485	485–565	600–780	
	loss/%	6.59	45.07	23.07	2.68	
	peak/°C	90 (endo)	290 (exo)	520 (exo)		
$Yb(L)_3 \cdot 3H_2O$	θ°C	30–140	140–480	480–580	580–750	
	loss/%	6.25	43.58	25.29	2.15	
	peak/°C	90 (endo)	290 (exo)	520 (exo)		
$Lu(L)_3 \cdot 3H_2O$	θ°C	30–14	140–155	455–530	530–720	
	loss/%	6.20	43.25	24.91	2.47	
	peak/°C	90 (endo)	290 (exo)	505 (exo)		
$Y(L)_3 \cdot 2H_2O$	θ°C	30–140	140–440	440–550	550–920	
	loss/%	4.56	44.43	31.44	4.10	
	peak/°C	90 (endo)	265 (exo)	495 (exo)	720 (exo)	

1589 cm^{-1} suggesting a $\nu_{anti\text{-}sym.}(COO^-)$ assignment, while the theoretical results show the corresponding peak at 1380 cm^{-1} with discrepancies –13.15%. (c) The third assignment shows a medium contribution at 1429 cm^{-1} suggesting a $\nu_{sym.}(COO^-)$ assignment, while the theoretical results show the corresponding peak at 1309 cm^{-1} with discrepancies –8.40%.

The simultaneous TG-DTA and TG/DTG curves of the compounds are shown in Fig. 2. This curves exhibit mass losses in four or five consecutive and/or overlapping steps and thermal events corresponding to these losses. Two patterns of thermal behaviour are observed up to 400°C. Firstly, a close similarity is noted concerning the TG-DTA profiles of europium and dysprosium compounds, Figs 2a and b. On the other hand gadolinium, terbium, holmium to lutetium and yttrium compounds display another set of very similar TG-DTA profiles. Due to the similarity between the patterns of the thermal behaviour, only the TG-DTA and TG/DTG curves of gadolinium, holmium and lutetium compounds are shown in Figs 2c, d and e. The same behaviour was also observed in the TG-DTA profiles of 2-Cl-BP compounds with lighter trivalent lanthanides [18].

These curves also show that the first mass loss for all the compounds occurs within the same temperature range (i.e. 30–140°C); the second mass loss also begins at the same temperature (140°C), showing that the thermal behaviour up to this step is not dependent on the nature of the lanthanide ion. However, the features shown by the next steps of thermal decomposition as well as the mass lost in each step are characteristic of each compound and no depend on the lanthanide ion present, as already observed for the same lanthanide and yttrium compounds with DMBP [12].

For all the compounds, the first mass loss between 30–140°C, corresponding to endothermic peaks at 88–95°C, is attributed to the dehydration, which occurs in a single step and through a slow process. This behaviour was also observed during the

dehydration of lanthanides and yttrium compounds with other phenyl-substituted derivatives of BP, and it seems to be characteristic of compounds obtained in amorphous state [11–15].

Once dehydrated, above 140 up to 580°C (Eu, Yb); 550°C (Gd, Tb, Dy, Tm); 530°C (Ho, Lu, Y) and 520°C (Er), the mass losses corresponding to exothermic events are attributed to oxidation of organic matter. For the europium and dysprosium compounds, the mass losses occur in three steps without a plateau between the steps. The similarity of TG-DTA curves up to this point suggests that the decomposition mechanism is the same for both compounds. For the other compounds (Gd, Tb, Ho–Lu, Y) the mass losses occur in two steps. The similarity among these curves also suggests that the decomposition mechanism should be the same for these compounds.

For all the compounds, the final residue up to this step was dissolved in nitric acid solution and did not indicate the formation of intermediate, oxy- or dioxycarbonate as observed in the thermal decomposition of lanthanides and yttrium compounds with 4-MeO-BP and DMBP [11, 12]. The non formation of these intermediates undoubtedly is due to the influence of the chloro- as phenyl substituted of BP, as already observed in the thermal decomposition of heavy trivalent

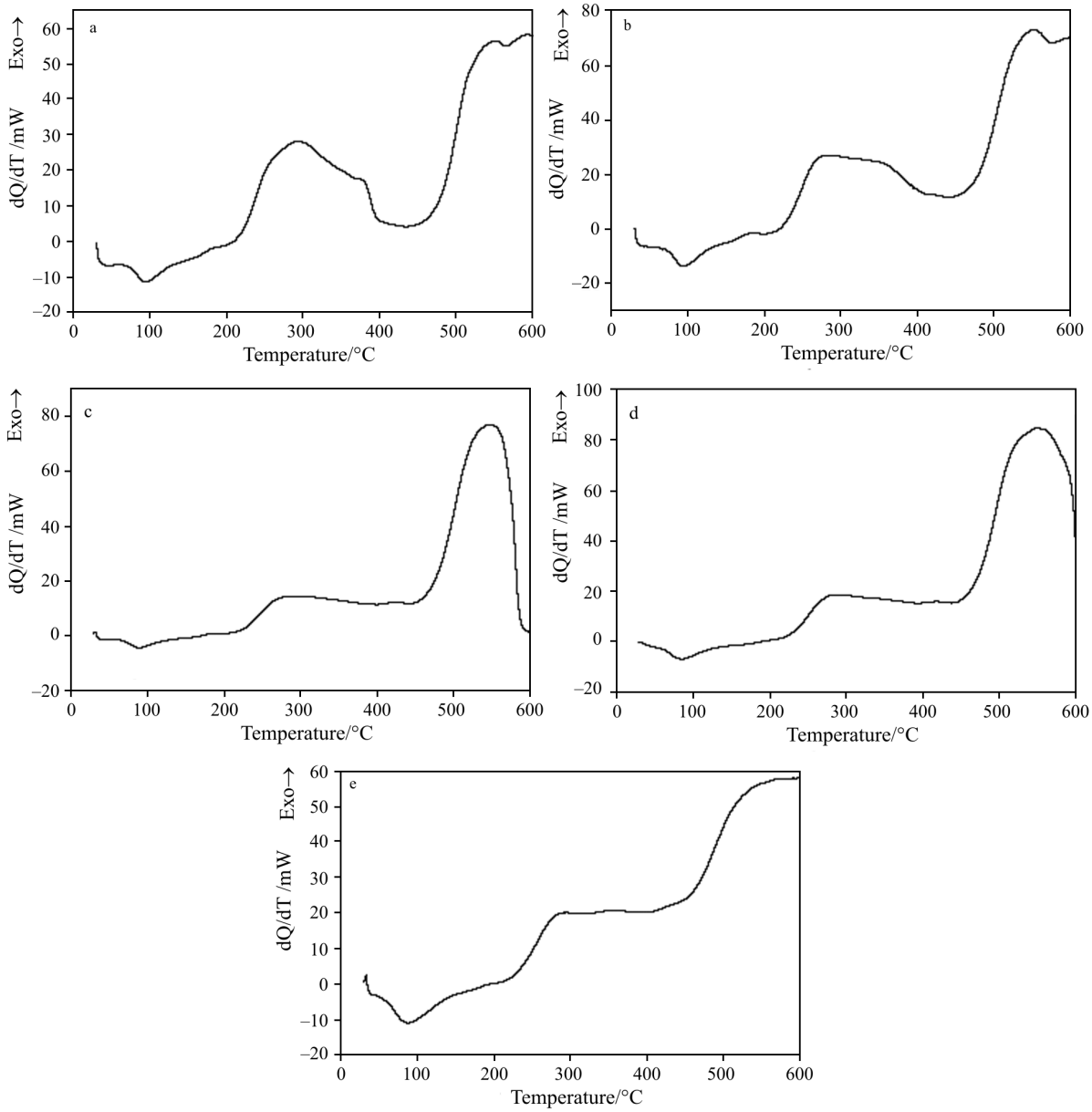

Fig. 3 DSC curves of the compounds: a – $Eu(2\text{-Cl-BP})_3 \cdot 2H_2O$ (m_i=5.2 mg), b – $Dy(2\text{-Cl-BP})_3 \cdot H_2O$ (4.7 mg), c – $Gd(2\text{-Cl-BP})_3 \cdot 2H_2O$ (4.9 mg), d – $Ho(2\text{-Cl-BP})_3 \cdot 3H_2O$ (5.3 mg) and e – $Lu(2\text{-Cl-BP})_3 \cdot 3H_2O$ (5.2 mg)

lanthanides and yttrium compounds with 4-Cl-BP [14]. Tests with $AgNO_3$ solution on these residues dissolved in nitric acid solution indicated the presence of chloride ions, and the X-ray powder patterns showed that the residue up to this temperature is a mixture of the respective metal oxide and oxychloride in no simple stoichiometric relation, and in agreement with [14, 18].

The last step between 700–1130 (Eu), 800–1170 (Gd), 750–980 (Tb), 700–1000 (Dy), 650–830 (Ho), 600–780 (Er), 600–780 (Tm), 580–750 (Yb), 530–720 (Lu) and 550–920°C (Y) is due to the thermal decomposition of lanthanide oxychloride to the respective oxide, Tb_4O_7 and Ln_2O_3 (*Ln*=Eu, Gd, Dy, to Lu and Y), as proven by their X-ray powder diffraction patterns, compared to those associated with the corresponding authentic oxides.

The mass losses, temperature ranges and the peak temperatures observed for each step of the TG-DTA curves are shown in Table 4.

The DSC curves of europium, dysprosium, gadolinium, holmium and lutetium compounds, as representative of the studied compounds are shown in Fig. 3.

As already observed in the TG-DTA curves, a great similarity is also observed in the DSC curves of europium and dysprosium compounds, as well as in the gadolinium, terbium, holmium to lutetium and yttrium compounds.

These curves show endothermic and exothermic peaks that all are in agreement with the mass losses observed in the TG curves. The endothermic peak at 88–95°C is assigned to the dehydration, which occurs in single step.

The dehydration enthalpies found for these compounds (Eu, to Lu and Y) were: 65.77, 55.63, 86.89, 121.65, 99.80, 109.59, 131.02, 119.78, 205.46 and 83.11 kJ mol^{-1}, respectively.

Conclusions

From TG curves, elemental analysis and complexometry results, a general formula could be established for these compounds in the solid-state.

The experimental and theoretical infrared spectroscopic data suggest that 2-Cl-BP acts as a bidentate ligand towards trivalent lanthanides and yttrium(III).

The TG-DTA, TG/DTG and DSC curves provided previously unreported information concerning the thermal behaviour and thermal decomposition of these compounds.

Acknowledgements

The authors thank FAPESP (Proc. 97/12646-8), CAPES and CNPq Foundations (Brazil) for financial support. Computational facilities of IQ-UNESP and CENAPAD-UNICAMP.

References

1 E. D. Stecher, M. J. Incorvia, B. Kerben, D. Lavine, M. Oen and E. Suhl, J. Org. Chem., 38 (1973) 4453 and references therein.
2 A. J. L. Cooper, J. Z. Ginos and A. Meister, Chem. Rev., 83 (1983) 321.
3 A. K. Datta and T. C. Daniels, J. Pharm. Sci., 52 (1963) 905.
4 W. Mayer, H. Rudolph and E. de Cleur, Angew. Makromol. Chem., 93 (1981) 83.
5 A. I. Baba, W. Wang, W. Y. Kim, L. Strong and R. H. Schmehl, Synth. Comm., 24 (1994) 1029.
6 G. Dujardin, M. Maudet and E. Brown, Tetrahedron Lett., 38 (1997) 1555.
7 G. Dujardin, S. Leconte, A. Bernard and E. Brown, Synlett, (2001) 147 and references therein.
8 C. B. Melios, V. R. Torres, M. H. A. Mota, J. O. Tognolli and M. Molina, Analyst, 109 (1984) 385.
9 C. B. Melios, J. T. S. Campos, M. A. C Mazzeu, L. L. Campos, M. Molina and J. O. Tognolli, Inorg. Chim. Acta, 139 (1987) 163.
10 R. N. Marques, C. B. Melios, N. C. S. Pereira, O. S. Siqueira, M. de Moraes, M. Molina and M. Ionashiro, J. Alloys Compd., 249 (1997) 102.
11 L. C. S. Oliveira, C. B. Melios, C. A. Ribeiro, M. S. Crespi and M. Ionashiro, Thermochim. Acta, 219 (1993) 215.
12 M. H. Miyano, C. B. Melios, C. A. Ribeiro, H. Redigolo and M. Ionashiro, Thermochim. Acta, 221 (1993) 53.
13 N. S. Fernandes, M. A. S. Carvalho Filho, C. B. Melios and M. Ionashiro, J. Therm. Anal. Cal., 59 (2000) 663.
14 N. S. Fernandes, M. A. S. Carvalho Filho, C. B. Melios and M. Ionashiro, J. Therm. Anal. Cal., 73 (2003) 307.
15 R. N. Marques, C. B. Melios and M. Ionashiro, Thermochim. Acta, 395 (2003) 145.
16 N. S. Fernandes, M. A. S. Carvalho Filho, R. A. Mendes, C. B. Melios and M. Ionashiro, J. Therm. Anal. Cal., 76 (2004) 193.
17 G. Bannach, E. Schnitzler, C. B. Melios and M. Ionashiro, Ecl. Quim., 29 (2004) 31.
18 G. Bannach, R. A. Mendes, E. Y. Ionashiro, A. E. Mauro, E. Schnitzler and M. Ionashiro, J. Therm. Anal. Cal., 79 (2005) 329.
19 E. Y. Ionashiro, F. L. Fertonani, C. B. Melios and M. Ionashiro, J. Therm. Anal. Cal., 79 (2005) 299.
20 M. Ionashiro, C. A. F. Graner and I. Zuanon Netto, Ecl. Quim., 8 (1983) 29.
21 C. C. J. Roothan, Rev. Mod. Phys., 23 (1951) 69.
22 J. S. Binkley, J. A. Pople and W. J. Hehre, J. Am. Chem. Soc., 102 (1980) 939.

23 Gaussian 98, Revision A.11.2, M. J. Frisch, G. W. Trucks, H. B. Schlegel, G. E. Scuseria, M. A. Robb, J. R. Cheeseman, V. G. Zakrzewski, J. A. Montgomery Jr., R. E. Stratmann, J. C. Burant, S. Dapprich, J. M. Millam, A. D. Daniels, K. N. Kudin, M. C. Strain, O. Farkas, J. Tomasi, V. Barone, M. Cossi, R. Cammi, B. Mennucci, C. Pomelli, C. Adamo, S. Clifford, J. Ochterski, G. A. Petersson, P. Y. Ayala, Q. Cui, K. Morokuma, N. Rega, P. Salvador, J. J. Dannenberg, D. K. Malick, A. D. Rabuck, K. Raghavachari, J. B. Foresman, J. Cioslowski, J. V. Ortiz, A. G. Baboul, B. B. Stefanov, G. Liu, A. Liashenko, P. Piskorz, I. Komaromi, R. Gomperts, R. L. Martin, D. J. Fox, T. Keith, M. A. Al-Laham, C. Y. Peng, A. Nanayakkara, M. Challacombe, P. M. W. Gill, B. Johnson, W. Chen, M. W. Wong, J. L. Andres, C. Gonzalez, M. Head-Gordon, E. S. Replogle, and J. A. Pople, Gaussian, Inc., Pittsburgh PA 2001.

24 F. A. Cotton, The Infra-Red Spectra in Metal Complex in Modern Coordination Chemistry (J. Lewis and R. G. Wilkins, Eds), Interscience, New York 1960, p. 379.

25 G. B. Deacon and R. J. Phillips, Coord. Chem. Rev., 33 (1980) 227.

26 D. Z. Goodson, J. Phys. Chem., 86 (1998) 659.

27 H. B. Schelegel, In new theoretical concepts for understanding organic reaction. J. Berdron, Ed., Academic, The Netherlands 1989, pp. 33–53.

Received: February 20, 2005
In revised form: May 26, 2005

DOI: 10.1007/s70973-005-6972-y